DOI: 10.1002/chem.200700577

The Nature of the $Ag^{I}\cdots Ag^{I}$ Interaction in Different $Ag(NH_3)_2$ Dimers Embedded in Supramolecular Solids

Shao-Liang Zheng,* Anatoliy Volkov, Cara L. Nygren, and Philip Coppens*[a]

Abstract: An isolated silver(I) ammonia monomer, a dimer, and a novel dimer containing an intercalated water molecule have been embedded as guests in supramolecular frameworks, $[Ag(NH_3)_2][(H_2thpe)(H_3thpe)]\cdot MeCN$ (**1**), $[\{Ag(NH_3)_2\}_2][(H_2thpe)_2]\cdot 4.25\,H_2O$ (**2**), and $[\{Ag(NH_3)_2\}\text{-}H_2O\text{-}\{Ag(NH_3)_2\}]\text{-}[(H_2thpe)_2]\cdot$benzene (**3**) ($H_3$THPE = tris(hydroxyphenyl)ethane). The $[\{Ag(NH_3)_2\}_2]^{2+}$ dimer is not stable as an isolated entity, but is stabilized by hydrogen bonding in the supramolecular framework. The water-intercalated silver(I) ammonia dimer, which constitutes a novel species, is also subject by hydrogen bonding in concentrated solutions. The destabilization energy of the dimer relative to isolated monomers is calculated to be $\approx 300\,kJ\,mol^{-1}$ by both perturbation methods and DFT theory. For the water-intercalated dimer it is calculated to be $\approx 200\,kJ\,mol^{-1}$ according to the BSSE-corrected MP2 calculation. The different aggregate states show a dramatic variation of absorption and emission properties, in accordance with the concentration dependent red-shift observed in solutions. Natural-bond-orbital analysis shows that the disilver-ammonium-aquo "sandwich" cation in **3** is stabilized by interaction between the π lone pair orbital on the oxygen atom of the water molecule and Ag^{I}–N σ antibonding molecular orbital.

Keywords: ab initio calculations · argentophilicity · crystal engineering · host–guest systems · luminescence

Introduction

The dilution of a photoactive guest in a periodic host environment is of importance in the study of photophysical properties and photoreactions in the solid state.[1–6] Unlike solutions or rigid glasses, which traditionally have been used to dilute photoactive species, the supramolecular solid state allows dilution without the loss of three-dimensional periodicity, and therefore, allows the application of diffraction methods to molecules embedded in cavities. The different aggregate states of entrapped molecules may result in a dramatic variation of the spectral properties, which can be related to the precisely determined molecular structure. We have shown that the xanthone molecule occurs as a monomer and as a dimer, respectively, in two crystalline resorcinarene-based frameworks,[2] the analyses of these showed a pronounced change in the spectral properties of the embedded molecules. Unlike the monomer, the dimer in the latter phase forms a phosphorescing triplet excimer on exposure to 366 nm light[7] that has a red-shifted emission compared with the monomer and a much longer emission lifetime (5.56 vs. 0.22 μs). The geometric differences in both the ground state and the excited state, accompanying the difference in luminescence behavior, may be studied by both conventional and time-resolved diffraction methods.[1,8,9] Time-resolved diffraction methods allow the identification of the excited species, and thus, interpretation of the photophysical properties at the atomic level.

Extensive attention has been focused on the attractive interactions existing between d^{10} closed-shell ions of group 11.[10,11] The term "aurophilicity" has been coined to describe gold(I)–gold(I) bonding interactions evident in many molecular and solid state structures. It has been attributed to correlation and relativistic effects.[10,11] The strength of aurophilicity (20–50 $kJ\,mol^{-1}$) is comparable to that of a typical hydrogen bond. It can be experimentally measured, and is large enough to affect the supramolecular structure; on the other hand, argentophilicity and cuprophilicity correspond to weaker interactions.[12,13] Similar to $Cu^{I}\cdots Cu^{I}$ interactions, the existence of ligand-bridged $Ag^{I}\cdots Ag^{I}$ interactions is supported by spectral evidence[14] and has been ex-

[a] Dr. S.-L. Zheng, Dr. A. Volkov, Dr. C. L. Nygren, Prof. Dr. P. Coppens
Department of Chemistry, State University of New York at Buffalo
Buffalo, New York, 14260-3000 (USA)
Fax: (+1) 716-645-6948
E-mail: chem9994@buffalo.edu
coppens@buffalo.edu

Supporting information for this article is available on the WWW under http://www.chemeurj.org/ or from the author.

amined by a series of theoretical calculations, which have sometimes reached different conclusions.[15] Most of the theoretical analysis of the $Ag^I\cdots Ag^I$ interactions are for neutral···neutral Ag^I dimers,[13,16,17] such as $[Ag(C_6F_5)\{N(H)=CPh_2\}]_2$,[13] or anion···anion dimers, such as $[\{Ag(CN)_2\}_2]^{2-}$,[18] in which the coordinating ligands are anionic. A recent comprehensive analysis[19] of $Cu^I\cdots Cu^I$ interactions has shown that in the ground state, often only a small part of the intermolecular interaction energy results from the $Cu^I\cdots Cu^I$ interaction, whereas even in the case of ligand-unsupported $Cu^I\cdots Cu^I$ species a large component is contributed by $Cu^I\cdots$ligand interactions.

In our preceding work we showed that an otherwise unstable ligand-unsupported Cu^I dimer can be stabilized in a supramolecular framework,[3] and a study of the geometry of unsupported $Au^I\cdots Au^I$ chains was carried out.[20] The current study concerns the structural and theoretical analysis of two Ag^I dimers that have neutral ligands, and their comparison with the monomeric structure. The solids synthesized contain an isolated silver(I) ammonia monomer, the corresponding dimer, and a solvent-separated dimer, all embedded in supramolecular frameworks, namely $[Ag(NH_3)_2]$-$[(H_2thpe)(H_3thpe)]$·MeCN (**1**), $[\{Ag(NH_3)_2\}_2][(H_2thpe)_2]$·4.25 H_2O (**2**), and $[\{Ag(NH_3)_2\}$-H_2O-$\{Ag(NH_3)_2\}]$-$[(H_2thpe)_2]$·benzene (**3**), (H_3THPE = tris(hydroxyphenyl)-ethane), respectively. Their syntheses, structures and photophysical properties are described below.

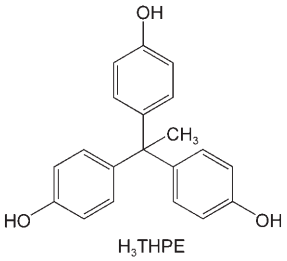

H_3THPE

Results and Discussion

Syntheses: $[Ag(NH_3)_2][(H_2thpe)(H_3thpe)]$·MeCN (**1**) was prepared by evaporation of an acetonitrile solution. No dimer phase could be obtained by this method, even though the composition of the corresponding reaction mixture and the solution were varied in a series of experiments.[21] However, $[\{Ag(NH_3)_2\}_2][(H_2thpe)_2]$·4.25 H_2O (**2**) that has a ligand-unsupported silver(I) dimer was occasionally obtained by hydrothermal synthesis,[21] similar to the process previously used to prepare isomorphous crystalline Cu^I compounds.[3] The crystallization conditions are highly influenced by the solvents used, the template, the pH value of the solution, and the steric requirements of the counterion.[4,22] Addition of salicylic acid to an aqueous solution stabilizes a dimeric configuration, as observed previously, and led to the desired product.[23] When a 1:1 aqueous ammonia/benzene mixture is used in the hydrothermal synthesis, a novel isolated solvent-bridged silver(I) dimer, $[\{Ag(NH_3)_2\}$-H_2O-$\{Ag(NH_3)_2\}][(H_2thpe)_2]$·benzene (**3**) is consistently produced.

Crystal Structures: Crystals of **1** contain two crystallographically independent H_3THPE molecules sharing one hydrogen (O(1)···O(6) 2.477(2) Å, Table S2 and Figure S1 in the Supporting Information). Adjacent $[(H_2thpe)(H_3thpe)]$ moieties are connected by intermolecular hydrogen bonds (O···O 2.654(2)–2.740(2) Å) to form a double layer parallel to the (101) plane (Figure 1). Adjacent hydrogen-bonded layers

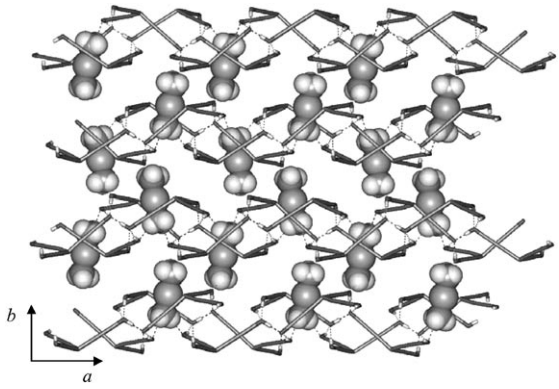

Figure 1. Three-dimensional supramolecular architecture of **1**, containing monomer $[Ag(NH_3)_2]^+$ viewed along the *c*-axis direction. The aromatic rings of H_2THPE are simplified by replacing the central part of the molecule by a line. The MeCN molecules are omitted for clarity.

are juxtaposed along the *b*-axis such as to leave a space parallel to the *a*-axis, accounting for 20.8 % of the overall crystal volume.[24] A fully isolated $[Ag(NH_3)_2]^+$ monomer (Ag–N 2.124(2) and 2.133(2) Å; N–Ag–N 178.06(7)°, Table S3) is entrapped within the space in each unit cell and hydrogen-bonded to the hydroxyl oxygen atom of the host network (N···O 3.058(2)–3.218(2) Å). One MeCN molecule per unit cell is clathrated to fill the remaining space.

There are two crystallographically independent H_2THPE anions in **2**, connected by hydrogen bonding (O···O 2.480(6) Å, Figures 2 and S2). The dimeric unit is further linked by hydrogen bonding to its symmetry related equivalent (symmetry code: −x+2, −y, −z+1) to form a two-dimensional wavy hydrogen-bonded layer (O···O 2.534(5)–2.572(5) Å) parallel to the (011) plane (Figure 2, top). Adjacent hydrogen-bonded layers are juxtaposed along the *b*-axis such as to leave smaller square-shaped channels (effective cross-section 2.1 × 2.1 Å) constituting 4.9 % of the crystal volume, as well as larger channels that have a 5.90 Å effective cross section accounting for 18 % of the crystal volume, both oriented parallel to the *a* axis.

Each of the larger channels contain two crystallographically independent Ag^I atoms per unit cell, each ligated by two ammonia nitrogen atoms (Ag–N 2.097(4)–2.110(3) Å; N–Ag–N 175.6(2) and 176.8(1)°, and separated by only 3.1417(4) Å, Figure 2, bottom). As this is significantly smaller than sum of the van der Waals radii (3.44 Å), they consti-

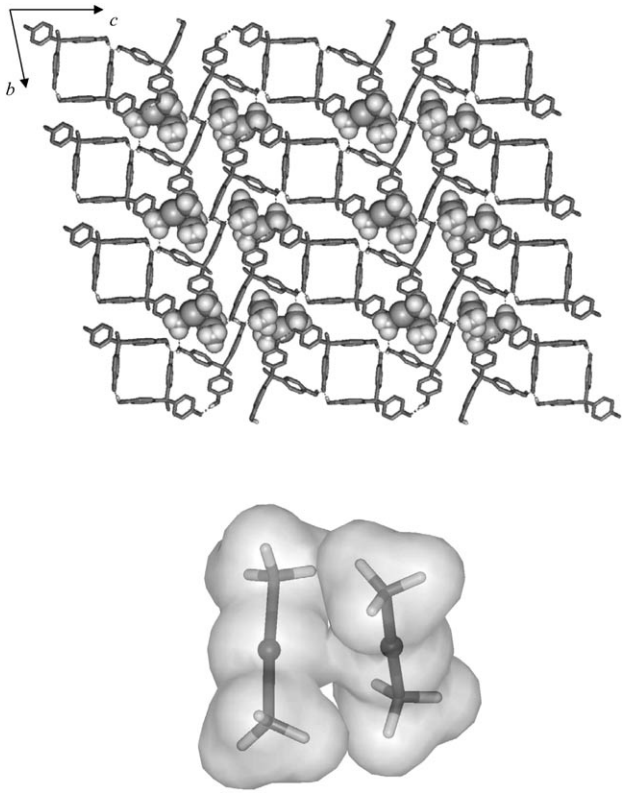

Figure 2. Three-dimensional supramolecular architecture of **2** (top) viewed along the *a*-axis direction (the water molecules included in the lattice are omitted for clarity). Shown at the bottom is the discrete dimeric $[\{Ag(NH_3)_2\}_2]^{2+}$ species (surfaces shown are defined by the atomic van der Waals radii).

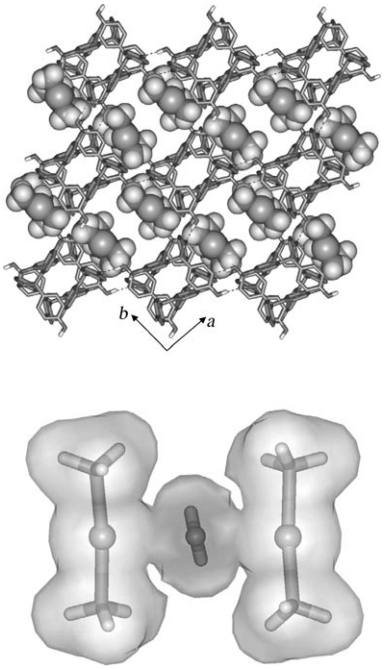

Figure 3. Three-dimensional supramolecular architecture of **3** (top) viewed along the *c*-axis direction, the benzene molecules are omitted for clarity. Shown at the bottom is the discrete dimeric $[\{Ag(NH_3)_2\}\text{-}H_2O\text{-}\{Ag(NH_3)_2\}]^{2+}$ species (surfaces shown are defined by the atomic van der Waals radii).

tute a dimeric $[Ag(NH_3)_2]_2^{2+}$ species. It is of interest that the N(3)–Ag(2)–N(4) angle of 175.6(2)° is such that the Ag(2) is displaced away from the other Ag atom, whereas Ag(1) is displaced in a direction perpendicular to the N(1)···Ag(2)···N(2) plane. Unlike the reported eclipsed $[Ag(NH_3)_2]_2^{2+}$ species, in which the $Ag^I\cdots Ag^I$ distance is larger (3.211(2) Å),[25] the N-Ag···Ag-N torsion angles are 72.9(2)° and 79.1(2)° for N(2)-Ag(1)···Ag(2)-N(3) and N(1)-Ag(1)···Ag(2)-N(4), respectively. The ammonia ligands act as donors in hydrogen bonds to the hydroxyl oxygen atoms of adjacent H_2THPE anions (N···O 2.855(5)–3.344(5) Å). One fully ordered water molecule is clathrated in each larger channel to fill the gap left between the Ag^I dimers. The water molecules are hydrogen bonded to the hydroxyl-oxygen atom of the host network (O(1W)···O 2.774(1) Å). The smaller square-shaped channels are occupied by disordered water molecules.

There is only one crystallographically independent H_2THPE anion in **3**. It is linked by hydrogen bonding to its related equivalents (O···O 2.527(5)–2.531(5) Å, Table S1 and Figure S3) to form a three-dimensional hydrogen-bonded ionic framework that has large channels parallel to the *c*-axis (effective dimensions 5.1×5.1 Å) constituting 43.8% of the crystal volume. The isolated solvent-separated dimer **3** (Figure 3), quite different from the silver(I) ammonia monomer in **1** or the dimer in **2**, is entrapped within each channel and is hydrogen bonded to the hydroxyl-oxygen atom of the host network (N···O 2.984(8)–3.114(7) Å). The Ag^I is ligated by two ammonia nitrogen atoms (Ag–N 2.110(6)–2.142(7) Å; N–Ag–N 172.2(2)°). The $[Ag(NH_3)_2]^+$ and its center-of-symmetry related equivalents (symmetry code: −x+2; y; −z+1/2) are connected by a solvent water molecule through weak Ag···O contacts (Ag···O···Ag 157.2(2)°, Ag(1)···O(1W) 2.776(1) Å), well beyond the values reported for other silver(I) complexes (2.33–2.62 Å).[26] The Ag^I atoms are separated by 5.442(1) Å and have N-Ag···Ag-N torsion angles of 32.5(2)°. In each channel, one disordered benzene molecule is clathrated to fill the remaining gap.

Molecular dilution: The most significant distinction amongst the three phases is that $[Ag(NH_3)_2]^+$ occurs as monomer in **1**, whereas it is a dimer in **2**, and it is a solvent-separated dimer in **3**. The molecular dilution of $[Ag(NH_3)_2]^+$ trapped in the supramolecular framework is pronounced. Its concentration in **1**–**3** is 1.781, 3.448, and 1.367 mol L^{-1}, respectively, compared with 12.597 mol L^{-1} for $[Ag(NH_3)_2]^+$ ions in neat $[\{Ag(NH_3)_2\}NO_3]$.[27]

Argentophilicity: Although **2** and its Cu^I analogue[3] are isomorphous, the $[\{Ag(NH_3)_2\}_2]^{2+}$ inclusion compound is much more difficult to obtain, even under hydrothermal conditions. Compared with the Cu^I analogue ($Cu^I\cdots Cu^I$ distance 3.0248(5) Å, Table S4), a slightly longer $Ag^I\cdots Ag^I$ contact (3.1417(4) Å) is observed in **2**, in contrast with earlier stud-

ies on the ligand-unsupported homologous Cu^I/Ag^I complexes, such as the dimer of dimers with a substituted phenanthroline/bipyridyl ligand,[16] and the dimer of trimers based on the substituted pyrazolates,[17,28] in which Ag···Ag contacts are shorter than the Cu···Cu distances. Notably, the neutral molecule-based silver(I) aggregates[16,17] are in fact large conjugate compounds that have strong intermolecular attractive dispersive Ag–π interactions.[29]

Calculations by Carvajal et al. have shown that bimolecular $Cu^I\cdots Cu^I$ aggregates that have like charges are not stable.[19] In the ground state often only a small part of the intermolecular interaction energy gained results from the direct $Cu^I\cdots Cu^I$ interaction, although a large component is contributed by $Cu^I\cdots$ligand interactions. The intermolecular perturbation theory (IMPT)[30] results show that in the $[\{Cu(NH_3)_2\}_2]^{2+}$ analogue, the electrostatic repulsion is dominant ($E_{el}=297.4\ kJ\,mol^{-1}$).[3] To gain insight into the $Ag^I\cdots Ag^I$ interactions, molecular orbital calculations were performed on the X-ray geometry of the $[\{Ag(NH_3)_2\}_2]^{2+}$ dimer. An IMPT calculation indicates that the Ag^I dimer in the geometry found in the crystals of **2** is less stable by $305.5\ kJ\,mol^{-1}$ than that in the isolated monomers (Table 2). The results are confirmed by BSSE-corrected MP2 calculations with Gaussion03, which give an $E_{el}=291.8\ kJ\,mol^{-1}$ and DFT calculations with ADF, which give $E_{el}=292.5\ kJ\,mol^{-1}$ (for details on the calculations see the Experimental Section). As in the Cu^I dimer studied by Carvajal et al., variation of the metal–metal distance shows no local minimum (Figure 4), this suggests that the observed dimer is unlikely to occur in diluted solution. Nevertheless, it can be stabilized in the supramolecular environment, as is evident from the crystal structure of **2**. As for the Cu^I dimer ($E_{el}=297.4\ kJ\,mol^{-1}$, Table 2), the electrostatic term in the Ag^I dimer is strongly repulsive ($E_{el}=292.7\ kJ\,mol^{-1}$). Therefore, it is important to take into account the electrostatic term when analyzing the nature of the interaction energy between the coinage metal atoms. An additional calculation of the electrostatic energy by means of the SPDFG program, which evaluates the electrostatic repulsion in terms of the monomer charge distributions,[31] confirms that in both cases the electrostatic repulsion is very large ($E_{el}=293.63$ and $278.23\ kJ\,mol^{-1}$ for the Cu^I and the Ag^I dimer, respectively). Nevertheless, the Mayer bond order[32] of $Ag^I\cdots Ag^I$ is calculated as 0.246 (Table 3), in agreement with the argentophilicity interactions investigated by spectroscopy that show the orbital interactions to be weakly attractive. The slightly longer $Ag^I\cdots Ag^I$ contact (3.1417(4) Å), relative to that of the Cu^I analogue (3.0248(5) Å), does not conflict with the result that Mayer bond order of $Ag^I\cdots Ag^I$ (0.246) is significantly larger than for the $Cu^I\cdots Cu^I$ interaction (0.181), as Ag^I is considerably larger than Cu^I (sum of the van der Waals radii for Cu 2.80 and Ag 3.44 Å).

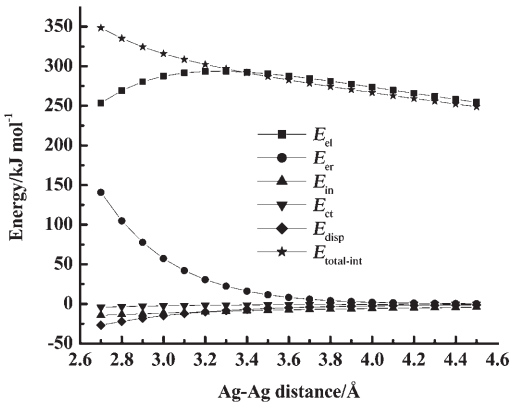

Figure 4. Variation of the IMPT total interaction energy ($E_{total\text{-}int}$) of $[\{Ag(NH_3)_2\}_2]^{2+}$ with Ag···Ag distance and its decomposition into Electrostatic (E_{el}), Exchange repulsion (E_{er}), Induction (E_{in}), Charge transfer (E_{ct}), and Dispersion (E_{disp}) interactions.

As in the Cu^I dimer, results of the DFT calculations, shown in Figure 5, indicate the HOMO-1 to be a $Ag^I\cdots Ag^I$ σ bonding-molecular orbital, the HOMO an $Ag^I\cdots Ag^I$ σ antibonding molecular orbital, and the LUMO to have $Ag^I\cdots Ag^I$ bonding character with 5d, 6s and 6p Ag^I contributions. Optimization of the excited triplet state gives a reduced $Ag^I\cdots Ag^I$ distance of 2.86 Å (Figure S4), indicating a much stronger metal–metal bonding interaction on the population of the $Ag^I\cdots Ag^I$ bonding LUMO, in accordance with the electronic structure of $[Ag(CN)_2^-]_n$, for which much stronger d^{10} metal–metal bonding and a possible formal metal–metal single bond has been predicted to exist in the electronically excited state.[18]

Table 1. Crystal data and structure refinement of **1**–**3**.

Compound	**1**	**2**	**3**
empirical formula	$C_{42}H_{44}AgN_3O_6$	$C_{40}H_{54.5}Ag_2N_4O_{10.25}$	$C_{46}H_{54}Ag_2N_4O_7$
formula weight	794.67	971.12	990.67
crystal system	monoclinic	triclinic	monoclinic
space group	$P2_1/n$ (No.14)	$P\bar{1}$ (No.2)	$C2/c$ (No.15)
a [Å]	13.1482(9)	6.9279(4)	16.0679(8)
b [Å]	19.7092(14)	12.0530(8)	18.2997(9)
c [Å]	14.4503(11)	23.9865(15)	17.4233(8)
α [°]	90	78.2209(13)	90
β [°]	94.8540(18)	89.1308(13)	108.4570(12)
γ [°]	90	79.3950(13)	90
V [Å^3]	3731.2(5)	1926.7(2)	4859.6(4)
Z	4	2	4
$\mu(Mo_{K\alpha})$ [mm^{-1}]	1.415	1.674	1.354
reflections collected	25713	24398	20373
independent reflections	8992	7527	4721
R_{int}	0.0344	0.0190	0.0330
goodness-of-fit on F^2	1.038	1.073	1.073
$R_1[I>2\sigma(I)]$	0.0305	0.0452	0.0725
wR_2(all data)	0.0766	0.1219	0.2129
$\Delta\rho_{max}/\Delta\rho_{min}$[e Å^{-3}]	1.191/−0.785	2.822/−1.374	3.173/−0.924

Table 2. Interaction energy ($E_{\text{total-int}}$) between two M^I monomers from IMPT, decomposed into five components: Electrostatic (E_{el}), Exchange repulsion (E_{er}), Induction (E_{in}), Charge transfer (E_{ct}), and Dispersion (E_{disp}).[a]

Dimer	E_{el}	E_{er}	E_{in}	E_{ct}	E_{disp}	$E_{\text{total-int}}$
$[Ag(NH_3)_2]_2^{2+}$	292.7	36.3	−10.5	−1.8	−11.3	305.5
$[Cu(NH_3)_2]_2^{2+}$[b]	297.4	35.4	−10.2	−2.1	−11.8	308.8

[a] Energy in kJ mol^{-1}. [b] The IMPT calculations with all-electron basis set consisted for Cu of the *p*VDZ basis set of Ahlrichs were reported in ref. [3]. To allow comparison of the silver, the parallel of IMPT calculations with all-electron basis set consisted for Cu of the DZVP basis set were re-performed here.

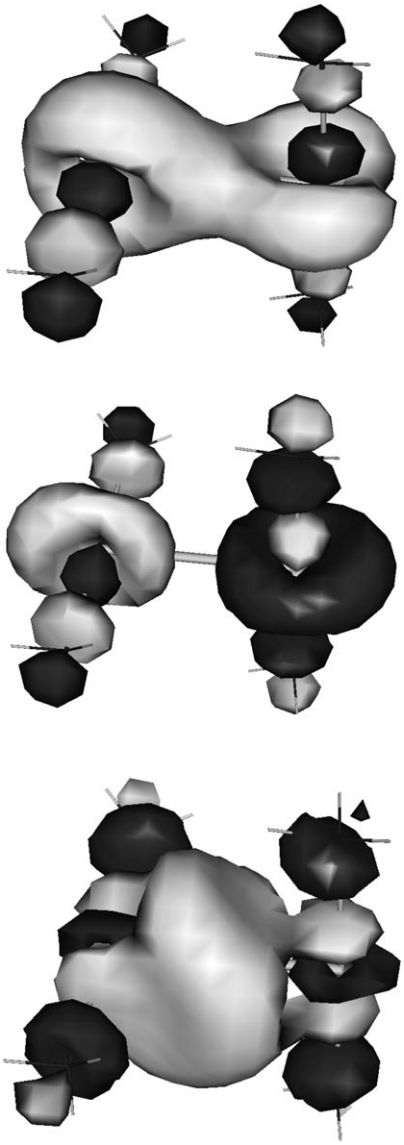

Figure 5. Contour plots (isosurfaces at ±0.04 au) of the frontier molecular orbitals of $[\{Ag(NH_3)_2\}_2]^{2+}$ in **2**: HOMO-1 (top), HOMO (middle), LUMO (bottom).

As the $[\{Ag(NH_3)_2\}_2]^{2+}$ dimer is unstable, it is not surprising that the solvent-separated dimer of **3**, $[\{Ag(NH_3)_2\}\text{-}H_2O\text{-}\{Ag(NH_3)_2\}]^{2+}$, can be obtained under different crystallization conditions. BSSE-corrected MP2 calculations show the total interaction energy between H_2O and $[\{Ag(NH_3)_2\}\cdots\{Ag(NH_3)_2\}]^{2+}$ to be $E_{\text{total-int}} = -9.90$ kJ mol^{-1}. Analysis of the natural bond orbitals shows an interaction between the π lone pair orbital on the oxygen atom of the water molecule and Ag^I–N σ anti-bonding molecular orbital (Figure 6). However, the total interaction energy [$\Delta E = E_{ABC}^{(ABC)} - E_A^{(ABC)} - E_B^{(ABC)} - E_C^{(ABC)}$] in $[\{Ag(NH_3)_2\}\text{-}H_2O\text{-}\{Ag(NH_3)_2\}]$ is calculated as $E_{\text{total-int}} = 206.4$ kJ mol^{-1} (BSSE-corrected MP2), again indicating the importance of electrostatic repulsions. Thus, this dimer must also be stabilized through interactions with the framework. The results of the DFT calculations, shown in Figure 7, indicate the canonical HOMO to be an $Ag^I\cdots Ag^I$ σ anti-bonding orbital, and the

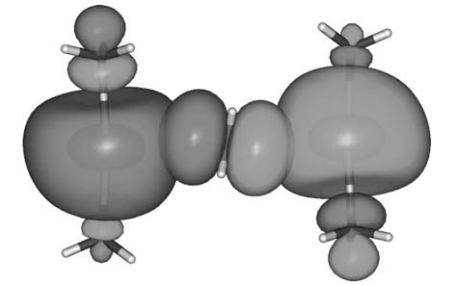

Figure 6. Contour plots (isosurfaces at ±0.04 au) of the natural bond orbital showing bonding between H_2O and $[\{Ag(NH_3)_2\}\cdots\{Ag(NH_3)_2\}]^{2+}$ in **3**.

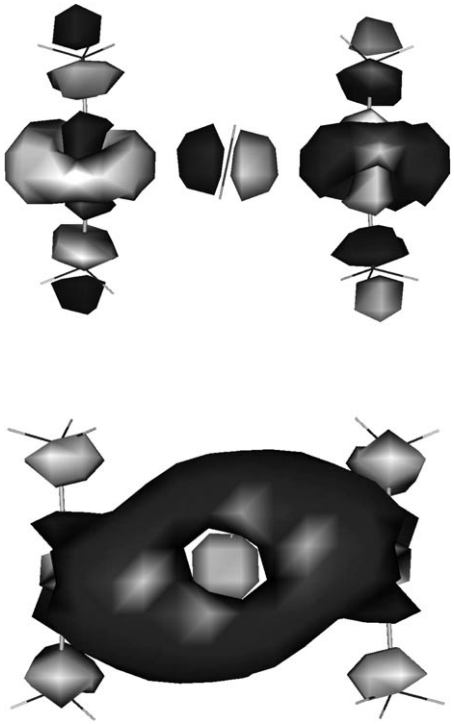

Figure 7. Contour plots (isosurfaces at ±0.04 au) of the frontier molecular orbitals of $[\{Ag(NH_3)_2\}\text{-}H_2O\text{-}\{Ag(NH_3)_2\}]^{2+}$ in **3**: HOMO (top), LUMO (bottom).

LUMO to have $Ag^I \cdots Ag^I$ bonding character with 5d, 6s and 6p Ag^I contributions. This suggests that the bonding for this ion may also be stronger in the excited state, as calculated for both $[\{Ag(NH_3)_2\}_2]^{2+}$ and $[\{Cu(NH_3)_2\}_2]^{2+}$, and observed for the latter.[1b]

Spectroscopic Properties: As shown by Patterson, Omary et al, the concentration-dependent red shift of the absorption edge of $[Ag(CN)_2^-]_n$ in solution is consistent with the orbital perturbation brought about by the $Ag^I \cdots Ag^I$ contacts.[18] The spectroscopic properties of the $[Ag(NH_3)_2]^+$ in the solid state similarly changes when the ions are in close contact. The strongest absorption bands of all three crystalline samples occur at 295 nm (Figure 8) and are attributed

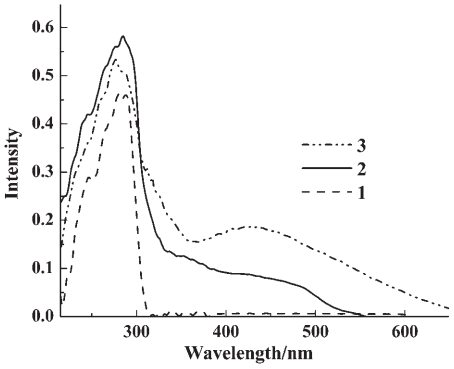

Figure 8. Solid state UV-Vis reflectance spectra of **1** (dashed line), **2** (solid line), and **3** (dashed/dotted line).

to the absorption of the THPE-based framework. Whereas **1** shows little absorption beyond this region, absorption bands centered at 430–450 nm are observed for **2** and **3**.

Individual analysis of neat crystals of **1** and H_3THPE show no significant emission on excitation even at 17 K.[33] However, the dimer in the crystals of **2** exhibits an intense emission at $\approx$530 nm that has a lifetime of 1.6 μs at 90 K, whereas the solvent-separated dimer in **3** exhibits a weak emission at $\approx$560 nm that has a lifetime of 1.2 μs at 90 K. The solid state is unique in that differences in absorption and emission behavior can be directly related to the unambiguously determined molecular aggregation. The dimers in **2** and **3** may equally occur in aqueous solutions, but may not be distinguishable from the solution spectra alone.[7]

Conclusion

We conclude that the aggregation of the silver(I) ammonia cation in the supramolecular solid state is strongly dependent on the method of preparation. As for Cu^I, the $[\{Ag(NH_3)_2\}_2]^{2+}$ dimer, which is not stable as an isolated entity, can be stabilized by hydrogen bonding in the supramolecular framework. The same is true for the water-intercalated silver(I) ammonia dimer, which constitutes a novel species, that likely will also occur in concentrated aqueous solutions. The destabilization of the dimer relative to isolated monomers is calculated at $\approx$300 kJ mol^{-1} by both perturbation methods and DFT theory, and $\approx$200 kJ mol^{-1} for the water-intercalated dimer according to the BSSE-corrected MP2 calculation. The different aggregate states show a dramatic variation of absorption and emission properties, in accordance with the concentration dependent red-shift observed in solutions.[18]

Molecular-dilution in supramolecular frameworks can be exploited not only in the study of weak interactions[2,3,34] in the ground state and in time-resolved diffraction studies of the excited state,[1] but also for the systematic analyses the dependence of spectroscopic properties on molecular aggregation.[2]

Experimental Section

Synthesis of $[Ag(NH_3)_2][(H_2thpe)(H_3thpe)]\cdot MeCN$ (1): A solution (5 mL) of H_3THPE (1.0 mmol) was added dropwise to a stirred MeCN solution (5 mL) of $AgNO_3$ (0.5 mmol) at 50 °C for 30 min. The mixture was dissolved by dropwise addition of an aqueous NH_3 solution. The resulting colorless solution was allowed to stand in air at room temperature for two weeks, yielding colorless crystals.

Synthesis of $[\{Ag(NH_3)_2\}_2][(H_2thpe)_2]\cdot 4.25H_2O$ (2): $AgNO_3$ (0.5 mmol), salicylic acid (0.5 mmol), H_3THPE (0.5 mmol), aqueous ammonia (25%, 2.0 mL), and water (2 mL) were sealed in a 6 mL Pyrex glass tube. The tube was allowed to stay at 120 °C for 1 hour, followed by cooling to room temperature over 40 h. Yellow needle-shaped crystals appeared during the cooling period.

Synthesis of $[\{Ag(NH_3)_2\}\text{-}H_2O\text{-}\{Ag(NH_3)_2\}][(H_2thpe)_2]\cdot$benzene (3): $AgNO_3$ (0.5 mmol), H_3THPE (0.5 mmol), aqueous ammonia (25%, 2.0 mL), and benzene (2 mL) were sealed in a 6 mL Pyrex glass tube. The tube was allowed to stay at 120 °C for 1 hour, followed by cooling to room temperature over 40 h. Orange needle-shaped crystals appeared during the cooling period.

X-Ray crystallography: Diffraction intensities for **1**–**3** were collected at 90 K by using a Bruker APEXII CCD diffractometer ($Mo_{K\alpha}$; λ = 0.71073 Å). The data were integrated, scaled, sorted, and averaged by using the SMART software package.[35] The structures were solved by direct methods and refined by means of full-matrix least-squares by using SHELXTL program package.[36] Anisotropic thermal parameters were applied to all nonhydrogen atoms. The hydroxyl and ammonia H atoms were located in difference maps, after which the riding model was applied (O–H: 0.84 Å; N–H: 0.91 Å). Aromatic hydrogen atoms and hydrogen atoms of the CH_3 group were positioned at idealized positions and refined in the same way. Crystal data as well as details of data collection and refinement for the complexes are summarized in Table 1, whereas hydrogen bond parameters, selected bond lengths and bond angles are listed in Table S2 and S3. Drawings were produced with Weblab Viewer Pro. 4.0.[37]

CCDC-604733–604735 contain the supplementary crystallographic data for this paper. These data can be obtained free of charge from the Cambridge Crystallographic Data Centre via

www.ccdc.cam.ac.uk/data_request/cif.

Theoretical calculations: Starting with the X-ray geometries, the X–H bond lengths were extended to the standard neutron diffraction distance ($O_{(water)}$–H 0.96 Å, N–H 1.009 Å).[38]

Table 3. Mayer bond orders in the $[Ag(NH_3)_2]^{2+}$ dimer.

Ag(1)···Ag(2)	0.246
Ag–N	0.516–0.528
N–H	0.826–0.849

All electron basis sets consisting of the DZVP basis set for Ag and the 3-21G basis set for the remaining atoms, were used in the IMPT analysis.[39]

The orbital analysis of the dimeric silver(I) species were based on calculations at the B88P86 level with TZP/O,N,H and TZ4P+/Ag basis sets, employing the ADF 2004 suite of programs.[40]

The BSSE-correlated MP2 calculations ($\Delta E = E_{AB}{}^{(AB)} - E_{A}{}^{(AB)} - E_{B}{}^{(AB)}$) were performed, employing the Gaussian 03 suite of programs.[41] The basis set used for light atoms was 6-31^{++}G**, whereas effective core potentials with a LanL2DZ basis set were employed for the Ag atom.

The new SPDFG program based on the numerical Rys quadrature method[42] has been discussed in ref. [31]. The molecular wave functions for Gaussian-type calculations were obtained with the Gaussian 03 suite of programs by using MP2 methods with DFT Dunning/H and WTBS/Ag,Cu,N basis sets.

Bond orders and valences[43] were obtained based on Gaussian 03 MP2 calculation results.

The contour plots of MOs were obtained with the Gabedit (Version 1.2.8) graphic program.[44]

UV-Vis reflectance and photoluminescence spectroscopy: UV-Vis absorption experiments were performed on a Perkin–Elmer Lambda 35 UV-Vis spectrometer equipped with an integrating sphere for diffuse reflectance spectroscopy. The spectra were collected in the 210–800 nm range at room temperature. Powdered crystals that were homogeneously diluted with a nonabsorbing matrix (MgO) and gently tapped into a sample holder were used as samples.

Photoluminescence measurements were carried out by using a home-assembled emission detection system. A single crystal sample was mounted on a copper pin attached to a DISPLEX cryorefrigerator. A metallic vacuum chamber with quartz windows is attached to the cryostat. The chamber was evacuated to approximately 10^{-7} bar by means of a turbomolecular pump, which allows cooling down to $\approx$17 K. The crystals were irradiated with 366 nm light from a pulsed N_2-dye laser. The emitted light was collected by an Oriel 77348 PMT device, positioned at 90° to the incident laser beam, and processed by a LeCroy Digital Oscilloscope that has a 1–4 GHz sampling rate.

Acknowledgements

Support of this work by the Petroleum Research Fund of the American Chemical Society (PRF32638 AC3) and the National Science Foundation (CHE0236317) is gratefully acknowledged.

[1] a) P. Coppens, B.-Q. Ma, O. Gerlits, Y. Zhang, P. Kulshrestha, *CrystEngComm* **2002**, *4*, 302–309; b) P. Coppens, S.-L. Zheng, M. Gembicky, M. Messerschmidt, P. Dominiak, *CrystEngComm* **2006**, *8*, 735–741.

[2] S.-L. Zheng, P. Coppens, *Chem. Eur. J.* **2005**, *11*, 3583–3590.

[3] S.-L. Zheng, M. Messerschmidt, P. Coppens, *Angew. Chem.* **2005**, *117*, 4690–4693; *Angew. Chem. Int. Ed.* **2005**, *44*, 4614–4617.

[4] a) B.-Q. Ma, L. F. Vieira Ferreira, P. Coppens, *Org. Lett.* **2004**, *6*, 1087–1090; b) S.-L. Zheng, P. Coppens, *CrystEngComm* **2005**, *7*, 289–293; c) S.-L. Zheng, P. Coppens, *Crys. Growth Des.* **2005**, *5*, 2050–2059; d) S.-L. Zheng, M. Gembicky, M. Messerschmidt, P. Dominiak, P. Coppens, *Inorg. Chem.* **2006**, *45*, 9281–9289.

[5] a) A. E. Keating, M. A. Garcia-Garibay in *Photochemical solid-to-solid reactions; Organic and inorganic photochemistry* (Eds.: V. Ramamurthy, K. S. Schanze), Marcel Dekker, New York, **1998**; b) *Topics in Current Chemistry, 254: Organic Solid State Reactions* (Ed.: F. Toda), Springer, **2005**, and references therein.

[6] a) S.-L. Zheng, M. Messerschmidt, P. Coppens, *Acta Crystallogr. Sect. B* **2007**, *B63*, 644–649; b) S.-L. Zheng, M. Messerschmidt, P. Coppens, *Chem. Commun.* **2007**, *26*, 2735–2737.

[7] a) N. N. Barashkov, T. V. Sakhno, R. N. Nurmukhanmetov, O. A. Khakel′, *Russ. Chem. Rev.* **1993**, *62*, 539–552; b) F. Brouwer in *Structure aspects of exciplex formation in Conformational analysis of molecules in excited states* (Eds.: J. Waluk), Wiley-VCH, **2000**, pp. 177–236, and references therein.

[8] a) P. Coppens, I. V. Novozhilova, *Faraday Discuss.* **2003**, *122*, 1–11; b) P. Coppens, *Chem. Commun.* **2003**, 1317–1320; c) P. Coppens, I. I. Vorontsov, T. Graber, M. Gembicky, A. Yu. Kovalevsky, *Acta Crystallogr. Sect. B* **2005**, *61*, 162–172.

[9] a) P. Coppens, I. I. Vorontsov, T. Graber, A. Yu. Kovalevsky, Y.-S. Chen, G. Wu, M. Gembicky, I. V. Novozhilova, *J. Am. Chem. Soc.* **2004**, *126*, 5980–5981; b) P. Coppens, O. Gerlits, I. I. Vorontsov, A. Yu. Kovalevsky, Y.-S. Chen, T. Graber, I. V. Novozhilova, *Chem. Commun.* **2004**, 2144–2145; c) I. I. Vorontsov, A. Yu. Kovalevsky, Y.-S. Chen, T. Graber, I. V. Novozhilova, M. A. Omary, P. Coppens, *Phys. Rev. Lett.* **2005**, *94*, 193003.

[10] a) P. Pyykkö, *Chem. Rev.* **1988**, *88*, 563–594; b) H. Schmidbaur, *Chem. Soc. Rev.* **1995**, *6*, 391–400; c) P. D. Harvey, *Coord. Chem. Rev.* **1996**, *153*, 175–198; d) P. Pyykkö, *Chem. Rev.* **1997**, *97*, 597–636.

[11] a) P. Pyykkö, *Angew. Chem.* **2004**, *116*, 4512–4557; *Angew. Chem. Int. Ed.* **2004**, *43*, 4412–4456; b) P. Pyykkö, *Inorg. Chim. Acta* **2005**, *358*, 4113–4130, and references therein.

[12] a) P. Pyykkö, N. Runeberg, F. Mendizabal, *Chem. Eur. J.* **1997**, *3*, 1451–1457; b) P. Pyykkö, F. Mendizabal, *Chem. Eur. J.* **1997**, *3*, 1458–1465.

[13] A. Codina, E. J. Fernandez, P. G. Jones, A. Laguna, J. M. Lopez-de-Luzuriaga, M. Monge, M. E. Olmos, J. Perez, M. A. Rodriguez, *J. Am. Chem. Soc.* **2002**, *124*, 6781–6786.

[14] a) C.-M. Che, S.-W. Lai *Coord. Chem. Rev.* **2005**, *249*, 1296–1309; b) D. L. Phillips, C.-M. Che, K.-H. Leung, Z. Mao, M.-C. Tse, *Coord. Chem. Rev.* **2005**, *249*, 1476–1490; and references therein.

[15] For example: a) F. A. Cotton, X. Feng, M. Matusz, R. Poli, *J. Am. Chem. Soc.* **1988**, *110*, 7077–7083; b) H. L. Hermann, G. Boche, P. Schwerdtfeger, *Chem. Eur. J.* **2001**, *7*, 5333–5342; c) L. Magnko, M. Schweizer, G. Rauhut, M. Schütz, H. Stoll, H.-J. Werner, *Phys. Chem. Chem. Phys.* **2002**, *4*, 1006–1013; d) E. O'Grady, N. Kaltsoyannis, *Phys. Chem. Chem. Phys.* **2004**, *6*, 680–687.

[16] a) X.-M. Zhang, M.-L. Tong, M.-L. Gong, H.-K. Lee, L. Luo, K.-F. Li, Y.-X. Tong, X.-M. Chen, *Chem. Eur. J.* **2002**, *8*, 3187–3194; b) J.-P. Zhang, Y.-B. Wang, X.-C. Huang, Y.-Y. Ling, X.-M. Chen, *Chem. Eur. J.* **2005**, *11*, 552–561.

[17] a) K. Singh, J. R. Long, P. Stavropoulos, *J. Am. Chem. Soc.* **1997**, *119*, 2942–2943; b) H. V. R. Dias, H. V. K. Diyabalanage, *Polyhedron* **2006**, *25*, 1655–1661; and references therein.

[18] a) H. H. Patterson, S. M. Kanan, M. A. Omary, *Coord. Chem. Rev.* **2000**, *208*, 227–241; b) M. A. Rawashdeh-Omary, M. A. Omary, H. H. Patterson, F. J. P. Jr. , *J. Am. Chem. Soc.* **2001**, *123*, 11237–11247; and references therein.

[19] a) M. A. Carvajl, S. Alvarez, J. J. Novoa, *Chem. Eur. J.* **2004**, *10*, 2117–2132; b) M. A. Carvajal, S. Alvarez, J. J. Novoa, *Theor. Chem. Acc.* **2006**, *116*, 472–479.

[20] S.-L. Zheng, C. L. Nygren, M. Messerschmidt, P. Coppens, *Chem. Commun.* **2006**, 3711–3713.

[21] A number of monomeric silver(I) ammonia monomer inclusion compounds, $[Ag(NH_3)_2][(H_2thpe)(H_3thpe)]\cdot n H_2O$ (n = 2, 2, and 0.5, CCDC reference numbers 604736–604738£, respectively, (see Table S1) were obtained.

[22] See for example: a) B. Moulton, M. J. Zaworotko, *Chem. Rev.* **2001**, *101* 1629–1658; b) S.-L. Zheng, M.-L. Tong, X.-M. Chen, *Coord. Chem. Rev.* **2003**, *246*, 185–202; c) S.-L. Zheng, J.-H. Yang, X.-L. Yu, X.-M. Chen, W.-T. Wong, *Inorg. Chem.* **2004**, *43*, 830–838.

[23] B. Coyle, M. McCann, K. Kavanagh, M. Devereux, V. McKee, N. Kayal, D. Egan, C. Deegan, G. J. Finn, *J. Inorg. Biochem.* **2004**, *98*, 1361–1364.

[24] PLATON, *A Multipurpose Crystallographic Tool*, L. Spek, Untrecht University, Utrecht, Netherlands, **2003**.

[25] S.-L. Zheng, M.-L. Tong, X.-M. Chen, S. W. Ng, *J Chem. Soc., Dalton Trans.* **2002**, 360–364.

[26] A. G. Orpen, L. Brammer, F. H. Allen, O. Kennard, D. G. Watson, R. Taylor, *J. Chem. Soc. Perkin Trans. 2*, **1989**, S1-S71.
[27] T. Yamaguchi, O. Lindqvist, *Acta Chem. Scand., Ser A* **1983**, *37*, 685–689.
[28] a) M. K. Ehlert, S. J. Rettig, A. Storr, R. C. Thompson, J. Trotter, *Can. J. Chem.* **1990**, *68*, 1444–1449; b) H. V. R. Dias, S. A. Polach, Z. Wang, *J. Fluorine Chem.* **2000**, *103*, 163–169; c) H. V. R. Dias, H. V. K. Diyabalanage, M. A. Rawashdeh-Omary, M. A. Franzman, M. A. Omary, *J. Am. Chem. Soc.* **2003**, *125*, 12072–12073.
[29] a) M. Munakata, L. P. Wu, G. L. Ning, *Coord. Chem. Rev.* **2000**, *198*, 171–186; b) S.-L. Zheng, J.-P. Zhang, W.-T. Wong, X.-M. Chen, *J. Am. Chem. Soc.* **2003**, *125*, 6882–6883.
[30] a) I. C. Hayes, A. J. Stone, *Mol. Phys.* **1984**, *53*, 83; b) *The Theory of Intermolecular Forces* (Ed.: A. J. Stone), Clarendon, Oxford, **1996**.
[31] A. Volkov, H. F. King, P. Coppens, *J. Chem. Theory Comput.* **2006**, *2*, 81–89.
[32] a) I. Mayer, *Chem. Phys. Lett.* **1983**, *97*, 270–274; b) I. Mayer, *Int. J. Quantum Chem.* **1984**, *26*, 151–154; c) A. J. Bridgeman, G. Cavigliasso, L. R. Ireland, J. Rothery, *J. Chem. Soc., Dalton Trans.* **2001**, 2095–2108.
[33] Lifetimes $< \approx 100$ ns, which is the detection limit of the equipment in our laboratory.
[34] A.-J. Zhou, S.-L. Zheng, Y. -Fang, M.-L. Tong, *Inorg. Chem.* **2005**, *44*, 4457–4459.
[35] SMART and SAINTPLUS-Area Detector Control and Integration Software, Madison, WI, **2004**.
[36] SHELXTL (6.10), G. M. Sheldrick, Bruker Analytical Instrumentation, Madison, Wisconsin, USA, **2000**.
[37] *Weblab Viewer Pro. 4.0*, Molecular Simulations, San Diego, USA, **1997**.
[38] F. H. Allen, O. Kennard, D. G. Watson, L. Brammer, A. G. Orpen, R. Taylor, *International Tables for Crystallography, Vol. C* (Eds.: A. J. C. Wilson) Dordrecht, Kluwer Academic Publishers, **1992**, pp. 685–706.
[39] a) I. C. Hayes, A. J. Stone, *Mol. Phys.* **1984**, *53*, 83; b) A. J. Stone, *The Theory of Intermolecular Forces*, Clarendon, Oxford, **1996**.
[40] G. te. Velde, F. M. Bickelhaupt, S. J. A. Van Gisbergen, C. Fonseca Guerra, J. G. Baerends, T. J. Ziegler, *J. Comput. Chem.* **2001**, *22*, 931–967.
[41] GAUSSIAN 03 (Revision C.02), M. J. Frisch, G. W. Trucks, H. B. Schlegel, G. E. Scuseria, M. A. Robb, J. R. Cheeseman, V. G. Zakrzewski, J. A. Jr., Montgomery, R. E. Stratmann, J. C. Burant, S. Dapprich, J. M. Millam, A. D. Daniels, K. N. Kudin, M. C. Strain, O. Farkas, J. Tomasi, V. Barone, M. Cossi, R. Cammi, B. Mennucci, C. Pomelli, C. Adamo, S. Clifford, J. Ochterski, G. A. Petersson, P. Y. Ayala, Q. Cui, K. Morokuma, D. K. Malick, A. D. Rabuck, K. Raghavachari, J. B. Foresman, J. Cioslowski, J. V. Ortiz, B. B. Stefanov, G. Liu, A. Liashenko, P. Piskorz, I. Komaromi, R. Gomperts, R. L. D. Martin, J. Fox, T. Keith, M. A. Al-Laham, C. Y. Peng, A. Nanayakkara, C. Gonzalez, M. Challacombe, P. M. W. Gill, B. Johnson, W. Chen, M. W. Wong, J. L. Andres, C. Gonzalez, M. Head-Gordon, E. S. Replogle, J. A. Pople, Gaussian, Pittsburgh, USA, **2003**.
[42] a) M. Dupuis, J. Rys, H. F. King, *J. Chem. Phys.* **1976**, *65*,111–116; b) J. Rys, M. Dupuis, H. F. King, *J. Comput. Chem.* **1983**, *4*, 154–157.
[43] BORDER (Version 1.0), I. Mayer, Chemical Research Center, Hungarian Academy of Sciences, Budapest, **2005**.
[44] Gabedit (1.2.8), A.-R. Allouche, **2002**, see http://lasim.univ-lyon1.fr/a.

Received: April 13, 2007
Published online: July 20, 2007

